

# Induced residual stresses in the preparation process of the glass-covered amorphous magnetic microwires

I. ASTEFANOAEI, D. RADU, H. CHIRIAC<sup>a</sup>

<sup>a</sup>“Al.I. Cuza” University, Faculty of Physics, Carol I Blvd., No. 11, RO-700050, Iasi, Romania

<sup>a</sup>National Institute of Research and Development for Technical Physics, 47 Mangeron Blvd., Iasi 3, Romania

In this paper we analyze the internal residual stresses that appear both during the solidification process and during cooling to the room temperature for a glass-covered amorphous magnetic microwire made from a *FeBSi*-type alloy, maintained at a constant temperature,  $T_w$ . We have proposed an improved theoretical method for calculation of the distribution of the internal stresses induced during both the solidification of the metal part and the cooling of the microwire, taking into account the difference between the thermal expansion coefficients of metal and glass. Theoretically obtained results are in very good agreement with the experimental data. The coupling between the positive magnetostriction and the stresses' distribution leads to an easy axes distribution associated with a magnetic domain structure consisting of a cylindrical inner core with axial magnetization (having the radius  $R_c \cong 94\%$  out of the metal part's radius) and a cylindrical outer shell with radial magnetization. If, in addition we consider the thermal stresses induced during the cooling process to the room temperature, then we found that the theoretical value of the magnetizations' ratio  $M_r / M_s$  is very close to the experimental one.

(Received March 15, 2006; accepted May 18, 2006)

**Keywords:** Residual stresses, Glass-covered amorphous microwires, Magnetic materials

## 1. Introduction

The aim of this paper is the evaluation of the thermal stresses during the solidification and cooling of an amorphous glass-covered microwire (AGCM) to the room temperature ( $T_w = 300\text{ K}$ ) considering both the thermal gradients that appear during the solidification of the metallic part and the thermal gradients that exist during the cooling of the material to the room temperature; we also consider the different thermal behaviour of the two materials (metal + glass) in contact.

In the description of the model presented in this paper we distinguish the following important tasks:

(i) The evaluation of the stresses that appear during the solidification process of the metallic part of AGCM;

(ii) The evaluation of the spatio-temporal distribution of the temperature during the forced cooling process to the room temperature. In this case we will analyze the spatial and temporal evolution of the temperature in the metal-glass system for different values of the AGCM diameter, considering the thermal boundary conditions at the metal-glass interface;

(iii) By knowing the spatio-temporal distribution of the temperature in AGCM one can obtain the stresses which appear both due to the forced cooling (because of the big thermal gradients) and to constraints produced on the metallic core by the glass cover as a result of the

difference between the thermal expansion coefficients of the two materials (metal and glass) in contact;

(iv) The calculation of the total stresses in AGCM and final discussions about the magnetic domains structure.

Table 1 shows the main AGCM characteristics.

## 2. Internal stresses induced in AGCMs

In this section we calculate the internal stresses induced in AGCMs due to the solidification and cooling processes of the sample, taking into account the difference between the thermal expansion coefficients of the two materials in contact (metallic core and glass cover). AGCMs consist in a cylindrical metallic core with a diameter of  $(3 \div 25)\mu\text{m}$ , covered by a glass insulation with a thickness of  $(2 \div 15)\mu\text{m}$  [1].

Let us consider an AGCM having the length  $L$ . We assume that the cylindrical metallic core of this AGCM has the radius  $R_m$ , and that the glass insulation has the thickness  $R_w - R_m$ ; here  $R_w$  is the total radius of the microwire (metal + glass). We associate a cylindrical system of coordinates  $(r, \theta, z)$  to the sample, having the  $Oz$ -axis along the microwire's axis (see Fig. 1).

Table 1. The main characteristics of the AGCM.

Characteristic quantity	Significance	Value
$c$	the specific heat of the metallic core	$530 \text{ J/kg K}$
$k_1$	the thermal conductivity of the metal part	$30 \text{ W/mK}$
$k_2$	the thermal conductivity of the glass cover	$1.177 \text{ W/mK}$
$\rho_M$	the mass density of the metal	$7.2 \cdot 10^3 \text{ kg/m}^3$
$\alpha_{metal}$	metal's thermal expansion coefficient	$8.7 \cdot 10^{-6} \text{ K}^{-1}$
$\alpha_{glass}$	glass' thermal expansion coefficient	$3.3 \cdot 10^{-6} \text{ K}^{-1}$
$E_{metal}$	Young's modulus of the metallic core	$2 \cdot 10^{11} \text{ N/m}^2$
$E_{glass}$	Young's modulus of the glass cover	$10^{11} \text{ N/m}^2$

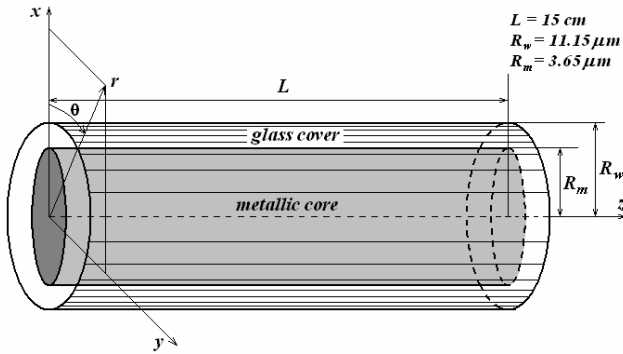


Fig. 1. The spatial orientation of the AGCM.  $R_m$  is the radius of the metallic core and  $R_w$  is the total microwire's radius.

## 2.1. The calculation of the internal stresses induced during the solidification of the metallic core

### i) The solidification process of the metallic core

In this section our aim is to analyze the solidification process of the metallic core of an AGCM; then, starting with the spatio-temporal distribution of the temperature during this process, one can determine the internal residual stresses induced in the sample. The internal energy of the material changes due to the heat losses through conduction, and the energy delivery through solidification. The samples' solidification takes place gradually, while the solidification front advances from the exterior to the interior of the melted material in the radial direction. According to the AGCM's preparation method (the rapid quenching from the melt – glass-coated melt spinning method) we consider that during its preparation process, the exterior surface of the microwire is maintained at a constant temperature equal to the room temperature,  $T_w = 300 \text{ K}$ . Let us denote by  $R_1 = R_1(t)$  the radius of the inner cylinder formed by the unsolidified material at a

certain moment  $t$ , by  $X(t)$  the “depth” (on the radial direction, from the microwire's surface to its core) where the solidification front reached at the moment  $t$ , and by  $R_m$  the radius of the metallic core of the AGCM. Obviously,  $R_1(t) = R_m - X(t)$ . The solidification process begins at  $t=0$ , when  $X(t=0)=0$  and  $R_1(t=0) = R_m$ . After a time  $t_s$ , the solidification front arrives in the metallic core's center, when the whole mass of melted material is solidified. We may write:  $X(t=t_s) = R_m$ ,  $R_1(t=t_s) = 0$ . The moment  $t$ , when the solidification front arrives at the surface of the cylindrical shell of radius  $r = R_1(t)$  “shares” the transverse surface of the microwire into two distinct zones. The first one corresponds to the already solidified material, while the second one corresponds to the material unsolidified yet. The two zones are connected through the solidification front. We consider that the solidification front temperature ( $r = R_1(t)$ ) is  $T_m = 1400 \text{ K}$  (the temperature of the melted material) and the material to be solidified finally reaches the room temperature,  $T_w = 300 \text{ K}$ . The spatio-temporal distribution of the microwire's temperature is determined by the Fourier equation of the heat transport [2]:

$$c_p \rho_m (\partial T / \partial t) = r^{-1} \partial [rk (\partial T / \partial r)] / \partial r, \quad (1)$$

where  $R_1(t) < r < R_m$ . In eq. (1)  $c_p$  is the specific heat,  $\rho_m$  is the mass density and  $k$  is the thermal conductivity of the material. The solution of eq. (1) with the following boundary conditions:

$$T(R_1, t) = T_m, \quad T(R_m, t) = T_g, \quad T(r, t=0) = T_m \quad (2)$$

represents the spatio-temporal distribution of the temperature in zone 2:

$$T(r, t) = \pi(T_m - T_g) \sum_{j=1}^{\infty} \frac{J_0^2(\alpha_j) Z_0(\alpha_j r / R_1) \exp[-a \alpha_j^2 t / R_1^2] + \frac{T_m \ln[R_m / r] + T_g \ln[r / R_1]}{\ln[R_m / R_1]}}{J_0^2(\alpha_j) - J_0^2(\alpha_j R_m / R_1)} \quad (3)$$

where

$$Z_0(\alpha_j r / R_1) = N_0(\alpha_j R_m / R_1) J_0(\alpha_j r / R_1) - N_0(\alpha_j r / R_1) J_0(\alpha_j R_m / R_1),$$

$J_0(pr)$  are the first order Bessel functions,  $N_0(pr)$  are the Neumann functions,  $a = k / (c_p \rho_m)$ , while

$\alpha_j \equiv p_j R_1$  are the roots of the characteristic equation:

$$J_0(\alpha) / [J_0(\alpha R_m / R_1)] = N_0(\alpha) / [N_0(\alpha R_m / R_1)].$$

### ii) The stresses due to the thermal gradients during the solidification process

We consider that the components of the displacement vector  $\vec{u}$  of any point of the microwire, namely  $u_r$ ,  $u_\theta$  and  $u_z$  are independent on/each other. Because of the

spatial symmetry of the solidification process, and implicitly of the displacements and strains generated by this process,  $u_\theta = \text{const.}$  in each point of the material. Because of this, we are interested only in the radial ( $u_r$ ) and axial ( $u_z$ ) components of the vector  $\vec{u}$ . The radial temperature gradients generate the radial ( $u_r^m$ ), axial ( $u_z^m$ ) and azimuthal ( $u_\theta^m$ ) displacements in the microwire, which lead to the following non-zero components of the stresses [3]:

$$\sigma_{rr}^m(x, \varepsilon) = \frac{\alpha_m E_m}{1-\mu} \frac{1}{x^2} \left\{ \left[ (x^2 - \varepsilon^2)/(1-\varepsilon^2) \right] \int_\varepsilon^1 xT(x)dx - \int_\varepsilon^x xT(x)dx \right\}, \quad (5.1)$$

$$\sigma_{\theta\theta}^m(x, \varepsilon) = \frac{\alpha_m E_m}{1-\mu} \frac{1}{x^2} \left\{ \left[ (x^2 + \varepsilon^2)/(1-\varepsilon^2) \right] \int_\varepsilon^1 xT(x)dx + \int_\varepsilon^x xT(x)dx - x^2 T(x) \right\}, \quad (5.2)$$

$$\sigma_{zz}^m(x, \varepsilon) = \frac{\alpha_m E_m}{1-\mu} \left\{ \left[ 2/(1-\varepsilon^2) \right] \int_\varepsilon^1 xT(x)dx - T(x) \right\}. \quad (5.3)$$

where  $E_m$  is the Young's modulus,  $\varepsilon = \varepsilon(t) = R_1(t)/R_m$  and  $x = r/R_m$ . The radial, azimuthal and axial stresses in a certain point  $x$ , ( $0 < x < 1$ ) result by integrating the expressions appearing in eqs. (5), *i.e.*:

$$\begin{aligned} \sigma_{rr}^m(x) &= \int_0^x \sigma_{rr}^m(x, \varepsilon) d\varepsilon, \quad \sigma_{\theta\theta}^m(x) = \int_0^x \sigma_{\theta\theta}^m(x, \varepsilon) d\varepsilon, \\ \sigma_{zz}^m(x) &= \int_0^x \sigma_{zz}^m(x, \varepsilon) d\varepsilon. \end{aligned} \quad (6)$$

*iii) The Stresses due to the compression of the interior shells by the exterior ones*

Due to the radial temperature distribution in the solid shell, the thermal stresses are induced inside the shell. These stresses are given by the relations (6). The exterior solid shell compresses the inner melted part of the microwire and so, during the solidification process, a corresponding pressure appears at the interface between the two zones (at the interface that separates the melted material and the solidified one); this pressure acts from the exterior to the inner shells. Using again the notations:  $x \equiv r/R_m$  and  $\varepsilon = \varepsilon(t) = R_1(t)/R_m$ , for the supplementary stresses (due to the compression) one can obtain the following expressions [4]:

$$\begin{aligned} \sigma_{rr}^s(x, \varepsilon) &= (p\varepsilon^2)(1-\varepsilon^2)^{-1}(1-x^{-2}), \\ \sigma_{\theta\theta}^s(x, \varepsilon) &= p\varepsilon^2(1+x^{-2})/(1-\varepsilon^2), \\ \sigma_{zz}^s(x, \varepsilon) &= 2p\varepsilon^2/(1-\varepsilon^2) \end{aligned} \quad (7)$$

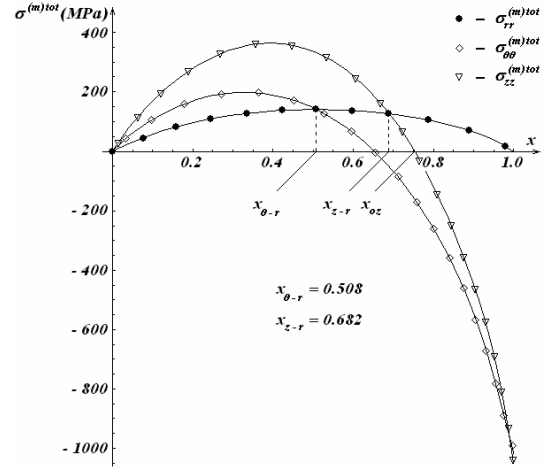


Fig. 2. The  $x$ -dependence of the total stresses (due to the thermal gradients and to the compression) induced in the metallic part of the AGCM.

By integrating, one can obtain:

$$\begin{aligned} \sigma_{rr}^s(x) &= \int_0^x \sigma_{rr}^s(x, \varepsilon) d\varepsilon, \\ \sigma_{\theta\theta}^s(x) &= \int_0^x \sigma_{\theta\theta}^s(x, \varepsilon) d\varepsilon, \\ \sigma_{zz}^s(x) &= \int_0^x \sigma_{zz}^s(x, \varepsilon) d\varepsilon. \end{aligned} \quad (8)$$

The pressure  $p$  exerted due to the solidification of the inner melted shell is determined by the compression of the whole solidified exterior shell, which is submitted to radial stresses due to the thermal gradients. Thus, we may write:

$$p \equiv p(x) = - \int_0^x \sigma_{rr}^m(x, \varepsilon) d\varepsilon,$$

where  $\sigma_{rr}^m(x, \varepsilon)$  is given by (5.1). The pressure  $p$  determined above is replaced into (7); these expressions are combined with (8), which give the stresses (radial, circumferential and axial), due to the compression. The total stresses in the microwire are obtained from the algebraic summation of the stresses due to the thermal gradients ( $\sigma^m$ ) and those due to the compression ( $\sigma^s$ ):  $\sigma^{(m)tot} = \sigma^m + \sigma^s$ . These total stresses are represented in Fig. 2.

## 2.2. Calculation of the internal stresses during the cooling process from $T_g$ to room temperature

*i) Temperature distribution in the AGCM*

*(a) temperature distribution in the metallic core*

In the following, we analyse the rapid cooling of the solidified metal from the temperature  $T_g$  to the room

temperature. As it will be shown, from a mathematical point of view, we may consider this as a problem of conduction and thermal transfer with a source, and it implies the determination of the spatio-temporal distribution of the temperature  $T_1(r, t)$  of the solidified material, which has in the center of the microwire the temperature  $T_g$ ; the source is distributed on the inner surface of the glass cover, having the temperature  $T_w$ . The heat losses in the alloy due to its forced cooling may be assimilated to some negative sources uniformly distributed. In the volume unity, the amount of sources is given by:

$$M = -2k_1(T_1 - T_w)R_m^{-1}.$$

The determination of the temperature  $T_1(r, t)$  implies to solve the equation of thermal balance for the material in the metallic part of the microwire, which is submitted to a rapid cooling process. Thus, from a mathematical point of view, this condition becomes:

$$\frac{\partial T_1}{\partial t} = a \left( \frac{\partial^2 T_1}{\partial r^2} + \frac{1}{r} \frac{\partial T_1}{\partial r} \right) - b(T_1 - T_w), \quad \text{for } 0 \leq r \leq R, \quad (1)$$

where  $a = k_1(\rho_m c_p)^{-1}$ ,  $b = k_1 PL(\rho_m c_p V)^{-1}$ ,  $P = 2\pi R_m$ , and  $L$  is the AGCM length. The general solution of this equation is of the form:

$$T_1(r, t) = T_w + C I_0\left(r\sqrt{(b/a) - n^2}\right) e^{-n^2 a t},$$

where  $C$  is an integration constant. By imposing the following "boundary" conditions,

$$\begin{cases} T_1(r=0, t=0) = T_g, \\ \left( \frac{\partial T_1}{\partial r} \right) \Big|_{r=0} = 0, \end{cases} \quad (2)$$

one can determine the constant  $C$ :  $C = T_g - T_w$ . We finally obtain the temperature distribution in the material:

$$T_1(r, t) = T_w + (T_g - T_w) I_0\left(r\sqrt{(b/a) - n^2}\right) e^{-n^2 a t}. \quad (3)$$

#### (b) temperature distribution in the glass cover

During the cooling process the glass cover receives the heat flux from the cooling metal. We will consider the temperature distribution in the glass cover of the form [4]:

$$T_2(r, t) = A_1 \ln(r) + A_2, \quad (4)$$

where  $A_1$  and  $A_2$  depend only on the time variable  $t$ :

$$A_1 \equiv A_1(t), \quad A_2 \equiv A_2(t).$$

#### (c) boundary conditions for the metal-glass interface

In order to determine the final expressions of the temperature,  $T_1(r, t)$  and  $T_2(r, t)$  we must use the following boundary conditions:

I) The heat flux from the metallic part is received by the glass cover. This heat flux must be continuous. So, for  $r = R_m$  we must have

$$k_1 \left( \frac{\partial T_1}{\partial r} \right) \Big|_{r=R_m} = k_2 \left( \frac{\partial T_2}{\partial r} \right) \Big|_{r=R_m}, \quad (5)$$

where  $k_1$  and  $k_2$  are the coefficients of thermal conductivity of the metal and glass cover, respectively;

II) On the metal-glass interface ( $r = R_m$ ), the temperatures of the adjacent regions must be equal:

$$T_1(r = R_m) = T_2(r = R_m); \quad (6)$$

III) The temperature on the outer surface of the AGCM, is equal to the room temperature, that is:

$$T_2(r = R_w) = T_w. \quad (7)$$

Using the boundary conditions given by (5) and (7) we obtain the following expressions for  $A_1$  and  $A_2$ :

$$A_1(t) = k_1 k_2^{-1} R_m (T_g - T_w) \left( \sqrt{(b/a) - n^2} \right) I_1 \left( R_m \sqrt{(b/a) - n^2} \right) \exp(-a n^2 t), \quad (8)$$

$$A_2(t) = T_w - k_2 k_1^{-1} R_m (T_g - T_w) \left( \sqrt{(b/a) - n^2} \right) I_1 \left( R_m \sqrt{(b/a) - n^2} \right) \ln(R_w) \exp(-a n^2 t) \quad (9)$$

and from conditions (6) we obtain the constant  $n$  as the solution of equation:

$$I_0 \left( R_m \sqrt{(b/a) - n^2} \right) = k_1 k_2^{-1} R_m \left( \sqrt{(b/a) - n^2} \right) I_1 \left( R_m \sqrt{(b/a) - n^2} \right) \ln(R_w R_m^{-1}) \quad (10)$$

The constants  $A_1$  and  $A_2$  have been calculated considering the characteristics given in Table 1. Solving the eq. (10) it results the constant  $n$  that help us to determine the spatio-temporal distribution of the temperature in AGCM. Fig. 3 (a) shows the spatio-temporal evolution of the temperature in the material of the microwire, which is subjected to forced cooling to the room temperature.

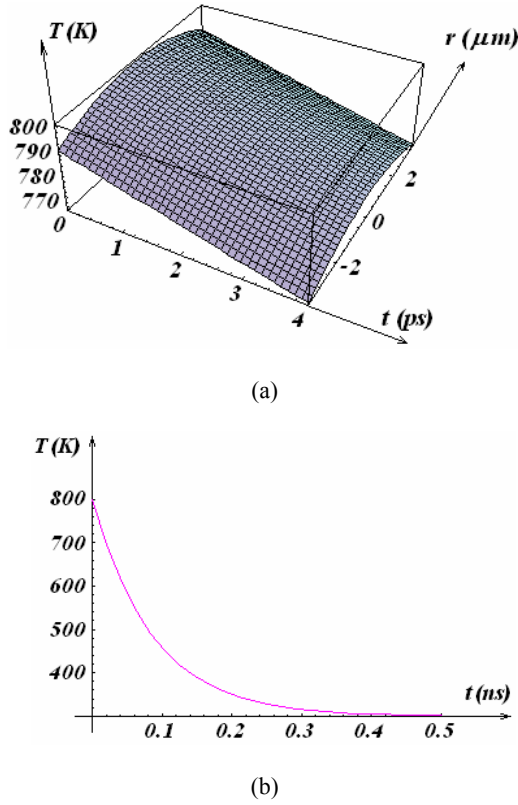


Fig. 3. The spatio-temporal distribution of the temperature in the metallic core of the AGCM.

Fig. 3 shows the spatio-temporal distribution of the temperature in the metallic core of the AGCM having the radius  $R_m = 3.65 \mu\text{m}$  and the thickness of the glass cover  $g = R_w - R_m = 7.50 \mu\text{m}$ . From this figure one can see that, concerning the radial distribution of the temperature, between the metallic core of the microwire and the metal-glass interface there is a temperature difference which is bigger in the first stages of the cooling process and smaller at the end of this process. Regarding the time evolution, (see Fig. 3(b)), the temperature decreases from  $T_g = 800 \text{ K}$  to the room temperature  $T_w = 300 \text{ K}$ , during the time interval of about  $0.4 \text{ ns}$ , measured from the end of the solidification process. In Fig. 4 we have presented the radial distribution of the temperature both in the cross-section of the metallic core (the red curves) and in the glass cover (the blue curves) at the three time moments, namely:  $t_1 = 0.1 \text{ ns}$ ,  $t_2 = 0.2 \text{ ns}$  and  $t_3 = 0.3 \text{ ns}$ , respectively. The temperature difference between the center of the metallic core and the metal-glass interface decreases with the time passing. For instance, for  $t_3 = 0.3 \text{ ns}$  we have  $\Delta T_{0R_m} = 0.27 \text{ K}$ , while for  $t_4 = 0.01 \text{ ns}$  we have  $\Delta T_{0R_m} = 7.72 \text{ K}$ . The radial distribution of the temperature in the glass cover is represented in Fig. 4. As one can see, after the time  $t_1 = 0.1 \text{ ns}$  from the end of the solidification process, the temperature difference between the metal-glass interface

and the exterior surface of the AGCM is of  $\Delta T_{R_m R_w} = 437 \text{ K}$ , while after the time  $t_3 = 0.3 \text{ ns}$  this difference is about  $\Delta T_{R_m R_w} = 15 \text{ K}$ .

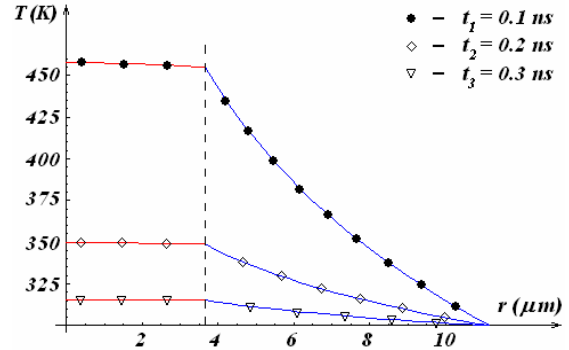


Fig. 4. The radial distribution of the temperature in the AGCM's cross-section after different moments ( $t_1 = 0.1 \text{ ns}$ ,  $t_2 = 0.2 \text{ ns}$  and  $t_3 = 0.3 \text{ ns}$ ).

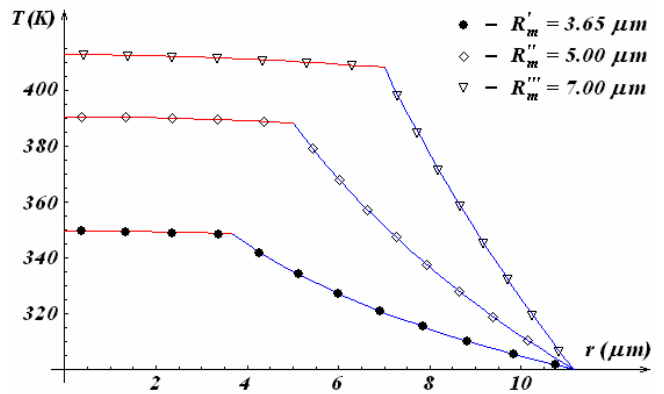


Fig. 5. The radial distribution of the temperature in the AGCM's cross-section (with  $R_w = 11.15 \mu\text{m}$ ), after the time  $t = 0.2 \text{ ns}$  for three values of the radius  $R_m$  ( $R_m' = 3.65 \mu\text{m}$ ,  $R_m'' = 5 \mu\text{m}$  and  $R_m''' = 7 \mu\text{m}$ , respectively)

The Fig. 5 shows the radial distribution of the temperature in the AGCM's cross-section (both in the metallic core of the microwire and in the glass cover) at the moment  $t_1 = 0.2 \text{ ns}$ , for three values of the radius of the metallic core:  $R_m' = 3.65 \mu\text{m}$ ,  $R_m'' = 5 \mu\text{m}$  and  $R_m''' = 7 \mu\text{m}$ , respectively. As one might have expected, after  $t = 0.2 \text{ ns}$ , the temperature in the core of AGCM, with the smaller radius of the metallic core ( $R_m' = 3.65 \mu\text{m}$ ) and the bigger glass cover thickness ( $g' = 7.50 \mu\text{m}$ ), is lesser than the temperature in the center of AGCM with the bigger metallic core's radius

( $R_m^m = 7 \mu m$ ) and the smaller glass cover's thickness ( $g^m = 4.15 \mu m$ ), as this last one is cooling slower. In the glass cover, one can observe that as its thickness gets smaller, the temperature's difference between the exterior surface of the microwire and the metal-glass interface  $\Delta T_{R_m, R_w}$  becomes larger, *i.e.*: for  $R_m^m = 3.65 \mu m$  ( $g^m = 7.50 \mu m$ ),  $\Delta T_{R_m, R_w} = 48 K$ , while for  $R_m^m = 7 \mu m$  ( $g^m = 4.15 \mu m$ ),  $\Delta T_{R_m, R_w} = 108 K$ .

*ii) The internal stresses which appear in the metallic core during the forced cooling process*

Let us analyze now the spatio-temporal distribution of the stresses which appear both due the thermal gradients and to the constraints produced on the glass cover by its ultra-rapidly cooling, as a result of the difference between the thermal expansion coefficients of the two materials in contact.

In order to obtain the stresses distribution during the cooling process of the AGCM, we will use the spatio-temporal distribution of the temperature presented in the above section.

The radial temperature gradients lead to the appearance of some displacements, both in the metallic core ( $u_r^{metal}$  and  $u_z^{metal}$ ) and in the glass cover ( $u_r^{glass}$  and  $u_z^{glass}$ ). These displacements satisfy the differential displacements' equation. In cylindrical coordinates, this equation reads [5]:

$$\frac{d}{dr} \left[ \frac{1}{r} \frac{d(u_r^{metal} r)}{dr} \right] = \frac{1+\mu}{1-\mu} \alpha_{metal} \frac{dT_1(r,t)}{dr}, \quad (11)$$

$$\left( du_z^{metal} / dz \right) = const., \quad (12)$$

for the metallic part and

$$\frac{d}{dr} \left[ \frac{1}{r} \frac{d(u_r^{glass} r)}{dr} \right] = 0, \quad (13)$$

$$\left( du_z^{glass} / dz \right) = const., \quad (14)$$

for the glass cover. In the above relations  $\alpha_{metal}$  is the alloy's thermal expansion coefficients,  $\mu$  is the Poisson's coefficient while  $T_1(r, t)$  is the spatio-temporal temperature distribution in the metallic core (3). It is assumed that the values of Poisson's coefficient for metal and glass cover are the same:  $\mu_{metal} = \mu_{glass} = \mu = 1/3$ . We will consider the influence of the constriction/dilatation effects, which exists due to the

different cooling of the two materials in contact (different dilatation coefficients), as well as the residual thermal stresses induced in the glass cover, due to these effects. The solutions of (11) – (14) equations (representing the radial,  $u_r^{glass}(r)$ , axial  $u_z^{glass}$  displacements in the metal,  $u_r^{metal}(r)$  and  $u_z^{metal}$ ) lead us to the following expressions of the stresses, first in the metallic part [6],

$$\sigma_{rr}^{metal}(r, t) = \frac{E_{metal}(C_1^m + 2\mu b_m)}{2(1+\mu)(1-2\mu)} - \frac{E_{metal}\alpha_{metal}}{r^2(1-\mu)} \int_0^r r T_1(r, t) dr, \quad (15.1)$$

$$\sigma_{\theta\theta}^{metal}(r, t) = \frac{E_{metal}(C_1^m + 2\mu b_m)}{2(1+\mu)(1-2\mu)} + \frac{E_{metal}\alpha_{metal}}{r^2(1-\mu)} \int_0^r r T_1(r, t) dr - \frac{\alpha_{metal} E_{metal} T_1(r, t)}{1-\mu}, \quad (15.2)$$

$$\sigma_{zz}^{metal}(r, t) = \frac{E_{metal}(C_1^m + 2\mu b_m)}{(1+\mu)(1-2\mu)} - \frac{\alpha_{metal} E_{metal} T_1(r, t)}{1-\mu}, \quad (15.3)$$

and then in the glass cover,

$$\sigma_{rr}^{glass}(r, t) = \frac{E_{glass}(C_1^l + 2\mu b_l)}{2(1+\mu)(1-2\mu)} - \frac{E_{glass} C_2^l}{(1+\mu)r^2}, \quad (16.1)$$

$$\sigma_{\theta\theta}^{glass}(r, t) = \frac{E_{glass}(C_2^l + 2\mu b_l)}{2(1+\mu)(1-2\mu)} + \frac{E_{glass} C_2^l}{(1+\mu)r^2}, \quad (16.2)$$

$$\sigma_{zz}^{glass}(r, t) = \frac{E_{glass}(C_1^l + 2\mu b_l)}{(1+\mu)(1-2\mu)}. \quad (16.3)$$

In order to determine the spatio-temporal distribution of the stresses both in the metallic part of AGCM and in the glass cover, we need to know the numerical values of the constants:  $C_1^m$ ,  $b_m$ ,  $C_1^l$ ,  $b_l$  and  $C_2^l$ . This can be done by imposing the boundary conditions that also take into account the different thermal behaviour of the two material in contact.

We will now calculate the resultant strain due to the cooling process of the two materials with different thermal expansion coefficients which are in contact during the entire process. The law of the linear thermal expansion is:  $l = l_0(1 + \alpha \Delta T)$ , where  $l$  is the linear dimension of the body in the chosen direction, at the temperature  $T$ ,  $l_0$  is the same linear dimension at the temperature  $T_0$ ,  $\Delta T = T - T_0$  is the temperature range in which the variation  $\Delta l = l - l_0$  takes place, and  $\alpha$  is the thermal expansion coefficient. In our case, for the metallic part of the microwire, we have:  $\varepsilon_{metal} = \alpha_{metal} \Delta T$ , and for the glass cover:  $\varepsilon_{glass} = \alpha_{glass} \Delta T$ , where  $\varepsilon_{glass}$  and  $\varepsilon_{metal}$  are the strains due to the thermal contraction in the metallic

part of the AGCM and in the glass cover, respectively, and  $\alpha_{glass}$  is the thermal expansion coefficient of the glass. The resultant strain is:  $\varepsilon = \varepsilon_{metal} - \varepsilon_{glass} = (\alpha_{metal} - \alpha_{glass})\Delta T$ . In this case,  $\Delta T$  is the difference between the  $T_g$  and the room temperature,  $T_w$ .

In order to determine  $\sigma_{rr}^{metal}(r, t)$ ,  $\sigma_{\theta\theta}^{metal}(r, t)$  and  $\sigma_{zz}^{metal}(r, t)$  we must find the values of the constants  $C_1^m$ ,  $b_m$ ,  $C_1^l$ ,  $b_l$  and  $C_2^l$ . The following conditions must be imposed on the metal-glass interface:

I) the strains that appear in this process result due only to the difference between the thermal expansion coefficients of the metal and glass:

$$u_r^{metal}(r = R_m) - u_r^{glass}(r = R_m) = \varepsilon R_m;$$

II) the equilibrium condition on the metal-glass interface:

$$\sigma_{rr}^{metal}(r = R_m, t) = \sigma_{rr}^{glass}(r = R_m, t)$$

III) the equilibrium condition on the exterior surface ( $r = R_w$ ) of the microwire:

$$\sigma_{rr}^{glass}(r = R_w, t) = 0.$$

Using these three conditions we can determine all the constants that appear in the expressions (15) and (16) of the stresses:

$$= \frac{(C_1^m + 2\mu b_m)}{2(1 + \mu)(1 - 2\mu)} = -\frac{E_{glass} R_m^2 (R_m^2 - R_w^2) \varepsilon (\mu - 1) + A \alpha_{metal} [E_{glass} (R_m^2 - R_w^2) (\mu + 1) + E_{metal} (R_m^2 - 3R_m^2 \mu + 2R_w^2 \mu)]}{R_m^2 (-1 + \mu) [E_{glass} (R_m^2 - R_w^2) (3\mu - 1) + E_{metal} (R_m^2 (1 - 3\mu) + 2R_w^2 \mu)]}$$

$$\frac{(C_1^l + 2\mu b_l)}{2(1 + \mu)(1 - 2\mu)} = \frac{E_{metal} (2A \alpha_{metal} - R_m^2 \varepsilon)}{E_{glass} (R_m^2 - R_w^2) (3\mu - 1) + E_{metal} (R_m^2 (1 - 3\mu) + 2R_w^2 \mu)},$$

$$C_2^l = \frac{E_{metal} R_w^2 (2 A \alpha_{metal} - R_m^2 \varepsilon) (\mu + 1)}{E_{glass} (R_m^2 - R_w^2) (3\mu - 1) + E_{metal} (R_m^2 (1 - 3\mu) + 2 R_w^2 \mu)},$$

where  $A = \int_0^{R_m} r T_1(r, t) dr$ . The explicit form of the stresses results by replacing the already determined constants in the relations (15) and (16).

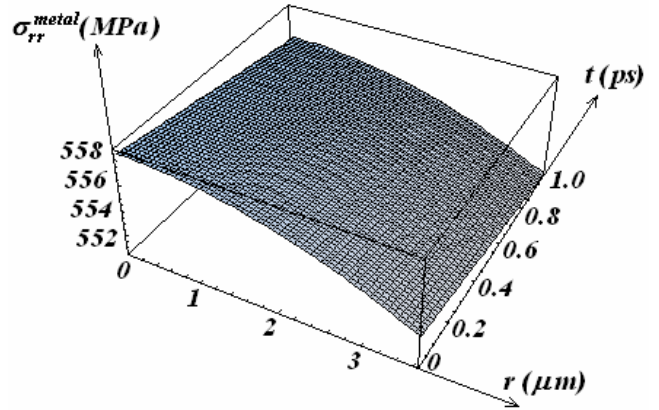


Fig. 6. The spatio-temporal distribution of the radial stresses in the metallic core of an AGCM having  $R_m = 3.65 \mu m$  and  $g = R_w - R_m = 7.50 \mu m$ .

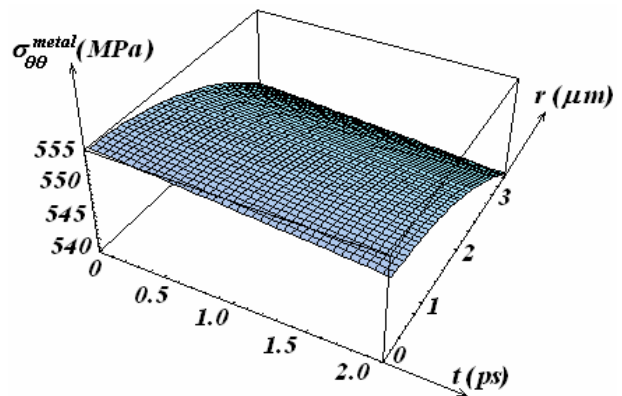


Fig. 7. The spatio-temporal distribution of the azimuthal stresses in the metallic core of an AGCM having  $R_m = 3.65 \mu m$  and  $g = R_w - R_m = 7.50 \mu m$ .

The Figs. 4, 5 and 6 show the spatio-temporal distributions of the radial, azimuthal and axial stresses in an AGCM having the radius of the metallic part of  $R_m = 3.65 \mu m$  and the thickness of the glass cover of  $g = R_w - R_m = 7.50 \mu m$ .

The spatio-temporal behaviour of the three stresses (radial, azimuthal and axial) after the time  $t = 0.02 ns$  from the complete solidification of the metallic core can be seen in Figs. 6, 7 and 8. We observe that the magnitude order of these stresses is  $10^8 Pa$ . As a common feature of the curves that represent the three stresses, we observe that they asymptotically tend to a saturation value which corresponds to the room temperature. This fact can be better observed in Fig. 9.

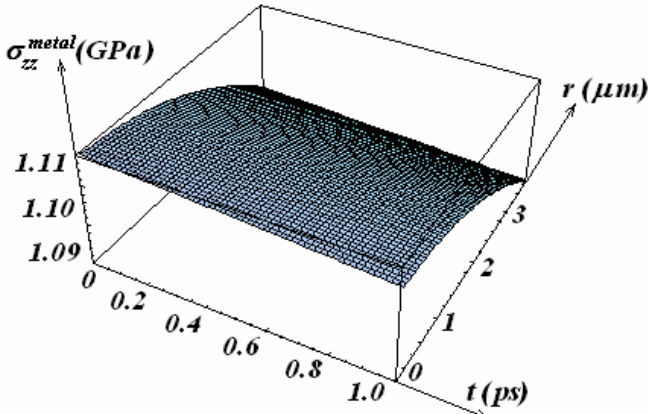


Fig. 8. The spatio-temporal distribution of the axial stresses in the metallic core of an AGCM having  $R_m = 3.65 \mu\text{m}$  and  $g = R_w - R_m = 7.50 \mu\text{m}$ .

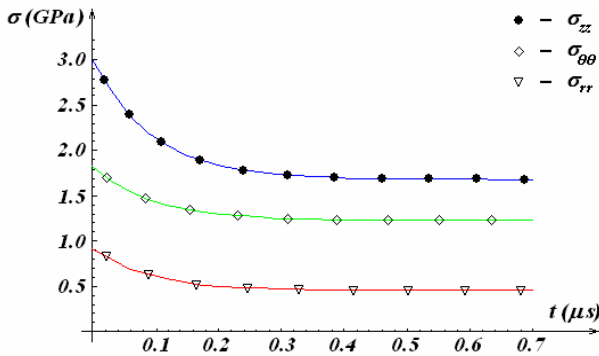


Fig. 9. The temporal evolution of the three stresses (radial, azimuthal and axial) in the point  $r = R_m$ .

In Fig. 9 one can observe at  $r = R_m$  that the axial stresses are approximately two times larger than the radial stresses. Moreover, the axial stresses obtain the saturation flat in a time shorter than for the other stresses. From Fig. 9 one can observe a relaxation of the stresses after the time interval  $t = 0.35 \mu\text{s}$ , when the sample has already reached the room temperature. The minimization of the stresses up to an approximately constant value in the temperature's interval  $(800 - 300) \text{K}$  shows us that the transformed (solidified) material has reached a much more regular structure. From eqs. (15) and (16), by analyzing the distribution of stresses in the metallic core of AGCM as functions of different radius of the AGCM, one can deduce that: the smaller the metallic core's radius, the bigger the stresses induced in this core.

### 2.3. The magnetic domains structure of AGCM. Results and discussion

In this subsection, we evaluate the total stresses in the AGCM from the algebraic summation of the stresses due to both solidification process  $\sigma^{(m)tot}$  and rapid cooling

from  $T_g$  to room temperature,  $T_w$ . These total stresses are represented in Fig. 10.

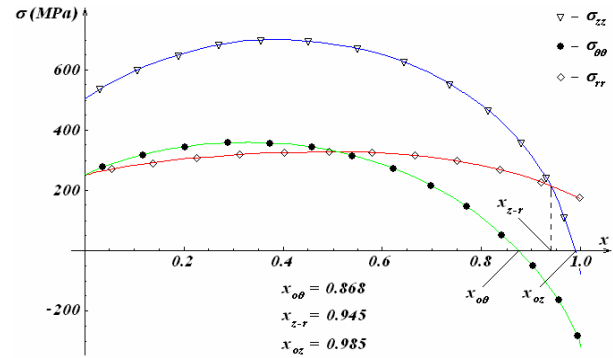


Fig. 10.  $x$ -dependence of the resultant radial, azimuthal and axial stresses induced in the AGCM.

As one can observe from Fig. 10, the total stresses distribution leads to a magnetic domains structure of the AGCM as follows: starting from the point  $x = 0$  up to the point  $x_{z-r} = 0.945$  there is a region in which  $\sigma_{zz}(x)$  is the component with the highest value and it is positive (zone I). From this point to the point  $x_{oz} = 0.985$  there is a second region, much narrower than the first one, in which  $\sigma_{rr}(x)$  is the highest positive stress component (zone II). The remaining part of the microwire constitutes a third region, dominated by the negative values (compression) of  $\sigma_{zz}(x)$  and  $\sigma_{\theta\theta}(x)$  (zone III).

As it is well known, the  $Fe_{77.5}Si_{7.5}B_{15}$  alloy is highly magnetostrictive ( $\lambda = 3 \cdot 10^{-5}$ ). This feature leads to a strong coupling (between the internal stresses and the magnetostriction) that determines the appearance in the AGCM of the easy axes of magnetization in the regions in which the dominant internal stresses are tensile (positive) and respectively, of the hard axes of magnetization in the regions in which the dominant stresses are compressive (negative). So, the magnetoelastic energy minimization leads to a domain structure which presents the following three zones:

- zone I:  $x \in [0, x_{z-r})$ ; due to the coupling between  $\sigma_{zz}(x)$  (positive) and the magnetostriction the first zone results, with an uniaxial magnetic anisotropy having the easy axis oriented along the axis of the AGCM ( $Oz$  - axis);

- zone II:  $x \in (x_{z-r}, x_{oz})$ ; due to the coupling between  $\sigma_{rr}(x)$  (positive) and the magnetostriction the second zone results, with a radial magnetic anisotropy. Also, in this zone the compressive component  $\sigma_{\theta\theta}(x)$  generates a hard axis of magnetization on the azimuthal direction;

- zone III:  $x \in (x_{oz}, 1]$ ; in this zone the two compressive components ( $\sigma_{\theta\theta}(x)$  and  $\sigma_{zz}(x)$ ) generate two hard axis of magnetization on the azimuthal direction and on the axial direction, respectively. Also, this zone presents a third (easy) axis of magnetization which appears because of the coupling between the  $\sigma_{rr}(x)$  (positive) and the magnetostriction.

Synthesizing, we can state that the stress distribution from Fig. 10, coupled with the high positive magnetostriction of the  $Fe_{77.5}Si_{7.5}B_{15}$  alloy, leads in a first order approximation to an easy axes distribution associated with a domain structure which consist of a cylindrical IC with axial magnetization (zone I) and an OS with radial magnetization (zone II plus zone III).

### 3. Experimental results

In order to verify by experimental means the above-obtained theoretical results, we have performed magnetic measurements on  $Fe_{77.5}Si_{7.5}B_{15}$  AGCMs by a fluxmetric method [7] in an alternating field having a maximum value of  $17.500 A/m$ , at  $200 Hz$ . We have measured the switching field  $H^*$  – that is the field at which the LBE appears – and the magnetization  $M^*$  at this field. For the considered microwire, the LBE occurs at  $H^* = 12 A/m$ , and we have found an experimental value of the ratio  $(M^*/M_s)_{exp}$  of 0.95. Using the relation [8]:

$$R_c / R_m = (M^* / M_s)^{1/2},$$

we have determined the experimental value of the fraction  $x_{z-r}^{exp} (\equiv r_{z-r}^{exp} / R_m)$  as being 0.975. The small difference between the theoretical evaluation  $\left[ x_{z-r}^{theor} = 0.945, (M^* / M_s)_{theor} = 0.89 \right]$  and experimental data [9],  $\left[ x_{z-r}^{exp} = 0.975, (M^* / M_s)_{exp} = 0.95 \right]$ , can be attributed to the supplementary axial tensile stresses induced in the preparation process of the AGCMs due to their continuous mechanical drawing. The good concordance between the experimental data and the theoretical results obtained in our paper represents an improvement with respect to big majority of the older models (see for example [10]).

### 4. Conclusions

The theoretical model described in this paper shows in a clear and synthetic manner the spatio-temporal distribution of the stresses induced in the metallic core of

an AGCM, during its cooling and solidification to the room temperature, considering both the thermal behavior of the metal and the supplementary stresses induced by the glass cover, due to the different cooling of the two materials in contact. We first analyzed the stresses appeared during the solidification of the metallic part of the AGCM, whose exterior surface is maintained at a constant temperature,  $T_w$ . The determination of these stresses implies the knowledge of the thermal behavior of the metal-glass system. In the thermal evolution of the metallic core, the longer the time interval from the beginning of the cooling process, the smaller the difference between the temperature in the center of the microwire and the temperature on the metal-glass interface. The center of the microwire “reaches” the room temperature,  $T_w = 300 K$ , in approximately  $t = 0.4 ns$  from the moment of the material’s solidification.

As the AGCM gets a bigger radius of the metallic core, the temperature in its center decreases more slowly. In the glass cover, one can deduce that, as its thickness becomes smaller, the temperature difference between the interior and the exterior surfaces,  $\Delta T_{R_m R_w}$ , becomes greater.

As for the stresses’s behavior, we deduced that the three stresses depend on the radius of the metallic core, being positive. The magnitude order of these stresses is  $10^9 Pa$ ; as a common feature, one can observe that all stresses tend toward a saturation value, corresponding to the room temperature. The decrease of stresses (their relaxation) up to an approximately constant value in the temperature interval  $(800 - 300) K$  shows us that the transformed (solidified) material has adopted a much more regular structure. The smaller the radius of the metallic core of AGCM, the bigger the stresses induced in the alloy.

Concerning the magnetic domains structure we have obtained the following results:

1) Starting from the point  $x = 0$  up to the point  $x_{z-r} = 0.945$  there is a region in which  $\sigma_{zz}(x)$  is the component with the highest value and it is positive (zone I). From this point to the point  $x_{oz} = 0.985$  there is a second region, much narrower than the first one, in which  $\sigma_{rr}(x)$  is the highest positive stress component (zone II). The remaining part of the microwire constitutes a third region, dominated by the negative values (compression) of  $\sigma_{zz}(x)$  and  $\sigma_{\theta\theta}(x)$  (zone III);

2) The small difference between the theoretical evaluation and experimental data, can be attributed to the supplementary axial tensile stress induced in the preparation process of the AGCM due to its continuous drawing.

### Acknowledgement

The authors wish to thank Romanian CEEEX POSTDOC-NANOSCIENCE and CNCSIS A-Consortium NANOCONS for the financial support of this research.

### References

- [1] M. Vázquez, D. X. Chen, IEEE Trans. Magn. **31**, 1229 (1995).
- [2] P. J. Schneider, Conduction Heat Transfer, Addison Wesley Publishing Company Inc. (1955).
- [3] L. Landau, E. Lifshitz, Physique Théorique, Tome 7- Théorie de l'élasticité, Mir Moscow (1990).
- [4] I. Aștefănoaei, D. Radu, H. Chiriac, Journal of Physics D: Applied Physics **38**, 235 (2005).
- [5] B. A. Bosley, J. H. Weiner, Theory of Thermal Stresses, Wiley, New York (1960).
- [6] S. G. Lekhnitskii, Theory of Elasticity of an Anisotropic Body, Ed. Mir Moscow (1977).
- [7] K. Mandal, S. K. Ghatak, J. Magn. Magn. Mater **118**, 315 (1993).
- [8] H. Chiriac, Gh. Pop, F. Barariu, M. Vázquez, J. Appl. Phys. **75**, 6949 (1994).
- [9] H. Chiriac, T.A. Óvári, Progress in Materials Science, 1998, p.32.
- [10] H. Chiriac, T.A. Óvári, Gh. Pop, Phys. Rev. **B 32**, 14 (1995).

---

\* Corresponding author: iordana@uaic.ro